Research Journal of Applied Sciences, Engineering and Technology 12(11): 1123-1129, 2016
DOI:10.19026/rjaset.12.2853
ISSN: 2040-7459; e-ISSN: 2040-7467

Submitted: October 31, 2015 Accepted: February 23, 2016 Published: June 05, 2016

Research Article

Numerical Study of Subgrade Humidity Field Evolution under Different Rainfall Infiltration Affected by Initial Water Contents

Zhijun Liu
State Key Laboratory for Geomechanics and Deep Underground Engineering, School of Mechanics and Civil Engineering, China University of Mining and Technology, Xuzhou 221116, Jiangsu, China

Abstract: To study the effects of initial water contents on subgrade humidity field distribution and evolution, 5 numerical models with different initial water contents are investigated in this study and the distributions of the subgrade humidity field affected by different initial water contents are obtained through the numerical rainfall infiltration test. The effects of different initial water contents on the humidity values of disturbed zone, extended distances and humidity gradients are also explored. The results show that the distribution and the change of the humidity fields caused by rainfall infiltration are affected by the initial water contents. The subgrade humidity of the same side of the disturbed zone increases linearly as the initial water contents increase and the further away from the slope surface, the larger the increase gradients are. The extended distance of the disturbed zone increase approximate linearly with the increase of the initial water contents. The higher the initial water content, the larger the infiltration coefficients and the faster the extend speeds. The disturbed zone can be divided into the front and the back zones. The humidity of the back zone is larger while the gradient is smaller than the front zone and the humidity gradient of the front zone decreases exponentially.

Keywords: Evolution rule, humidity field, initial water content, numerical experiment, subgrade engineering

INTRODUCTION

Water damage, one of the most common issues in subgrade engineering, is often caused by the change of the humidity fields due to the outside water infiltration, which degrades the mechanical property of the subgrade (Tarefder *et al*., 2010). Rainfall infiltration is the most common form of outside water. Therefore, the study of the subgrade humidity field evolution under rainfall infiltration is of great importance (Liu, 2012). The subgrade humidity keeps at a relative balanced level in the dry seasons and differs from each other due to the specific engineering conditions of the highway (Zuo *et al*., 2002; Heydinger and Davies, 2006). However, under the strong rainfall infiltration in the rainy seasons, the humidity fields change sharply. Therefore, under same rainfall condition, the evolution of the subgrade humidity field from its initial state, is expected to be further studied.

Zhang and Song (2011) studied the dynamic change of the water content with the increase of the infiltration time under the same water head and the same initial water content in a one-dimensional infiltration experiment.

Mahmood and Kim (2011) investigated the reliability of the unsaturated subgrade under rainfall infiltration by measuring the distribution of the matric suction of the slope cross section in a period of time under different rainfall intensity.

Zeng *et al*. (2012) studied the slope stability of the carbonaceous mudstone road under the rainfall infiltrations through numerical simulations. The results show that the initial state of the negative pore water pressure of carbonaceous mudstone embankment slope surface layer gradually extends to positive pore pressure under the action of rainfall. At the same time, volumetric moisture content in the transient saturated zone of the slope reaches saturated, along with the forming of the transient saturated zone.

Mahmood *et al*. (2013) studied the anisotropy of the osmotic coefficient in the unsaturated zone by establishing a subgrade numerical model with different anisotropic conductivity ratios. In this model, the depth of the groundwater was 7m and the slope surface was taken as the osmotic surface and the rainfall intensity was $3.5*10^{-6}$m/s in 66 hours. The distribution of the pore pressure or the water contents of the vertical fracture surface of the road shoulder was analyzed. The results show that during the rainfall, the soil in the unsaturated zone remains unsaturated as the wetting front moves through it. The wetting front is deeper for lower ratios. The rainwater reaches the ground water

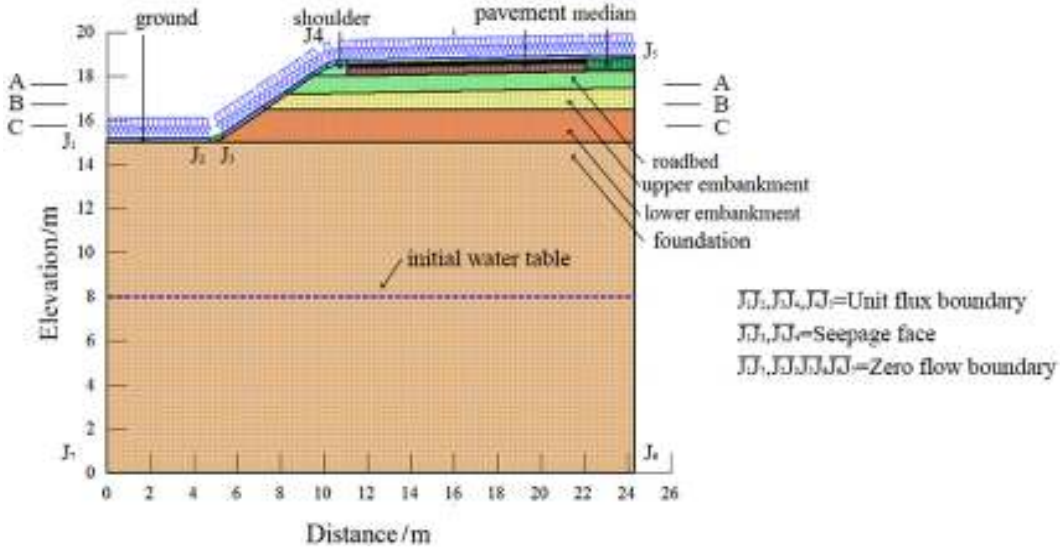

Fig. 1: Numerical model of subgrade humidity field

Table 1: Initial water contents of the model

	Model number				
Humidity index	1	2	3	4	5
Mass water fraction /%	3	5	7	9	11
Volumetric water content /(m³/m³)	0.075	0.119	0.159	0.196	0.230

level within a short time and has significant effect on the pore-water pressure profile.

Cho and Lee (2001) studied the change of the pore pressure in the slope with initial groundwater and the rainfall intensity was 20mm/h in 66 hours, the distribution nephogram of the slope pore pressure after the rainfall was obtained through the numerical experiment. The results show that the initial groundwater depths increase due to the disturbance during the rain and the rainfall infiltrations expand from the top, surface to the bottom of the slope, following a U shape curve. The studies mentioned above are all based on the subgrade models which consider the influence of the rainfall intensity, rainfall duration and groundwater depth on the humidity field. The author also investigated the influence of the compactness on the subgrade humidity field evolution under the rainfall condition in previous studies (Liu, 2014, 2015) and the subgrade model was divided into different compacted zones according to the real condition. In this study, the evolution rule of the humidity fields under the influence of the initial water content based on the actual compacted zones is further studied to provide theory references on the prevention of water damage.

NUMERICAL EXPERIMENT DESIGN

The SEEP\W, professional soil seepage numerical finite element analysis software, was adopted in this study to build different models.

The top width of the subgrade model is 13 m and the height of the subgrade is 3 m and the depth of the foundation is 15 m. The slope rate is 1:1.5. The subgrade is divided into roadbed, the upper embankment, the lower embankment and the subgrade zones whose compactness degree are 96, 94, 93 and 93%, respectively. Only half range of the cross section of the subgrade was modeled due to the symmetry. The model is divided into 7,434 elements and 7,592 nodes.

The related boundary conditions in the experiment are as follows:

The rainfall intensity is 144 mm/d during a four-day rainfall. The initial groundwater depth is 7m under the surface. The road, shoulder and the intermediate zone are watertight (The surface layer material is set to null). The infiltration surfaces are defined as the slope and the foundation outside the slope. Ditches at the slope toe were set and there had no rain (Fig. 1).

The 5 models with different initial water contents are shown in the Table 1.

In the numerical test, the locations chosen to record the subgrade humidity were 30-cm (A-A), 120-cm (B-B), 250-cm (C-C) below the roadbed top surface (representing the roadbed, the upper embankment and the lower embankment respectively).

TEST RESULTS AND DISSCUSSION

Soil physical properties and water movements: Soil used in the experiment is the silty clayey soil.

According to the physical test results, liquid limit, plastic limit, plasticity index IP, optimum water content and maximum dry density of the soil sample are 35.9, 21.0, 14.9 11.6, 1.87 g/cm^3, respectively and the soil particle sizes are shown in Table 2.

The relationship of water conductivity k and matric suction Ψ under different compactness, fitted by the SEEP/W, is shown in Fig. 2a, while the water characteristic curve, namely the relationship between water content θ and matric suction Ψ, under different compactness, is shown in Fig. 2b, according to the Van Genuchten model.

Subgrade humidity field evolution: After 4 days of rainfall experiment, the contours of the subgrade humidity field under different initial groundwater levels are shown in Fig. 3.

In Fig. 3, the rainfall infiltration formed a humidity disturbed area. The humidity isolines expand toward the inner part of the subgrade, making the humidity of the area between the slope and humidity summit differ from that of the area with initial water content. Meanwhile, the distributions of the disturbed area are different as the result of the initial water content disturbance. In general, the range of the disturbed area increases as the initial water content increases. The distributions of subgrade humidity changed with different initial water contents at the observation locations are shown in Fig. 4.

Under the influence of initial water contents, the humidity field evolution presents the following characteristics.

Change of the subgrade humidity: After the rainfall infiltration, the humidity of the slope surface is the

Table 2: Soil grain size analysis

	Grain size /mm						
Index	10	5	2	1	0.5	0.25	0.075
Particles smaller than the grain size/%	100	100	99.8	99.4	81.4	73.2	42.9

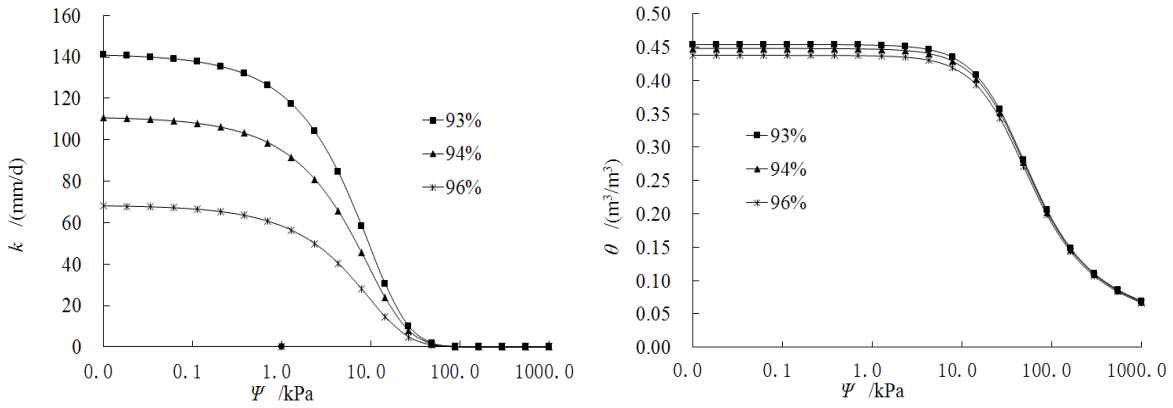

(a) (b)

Fig. 2: Soil water movement curves; (a): k~Ψ; (b): θ~Ψ

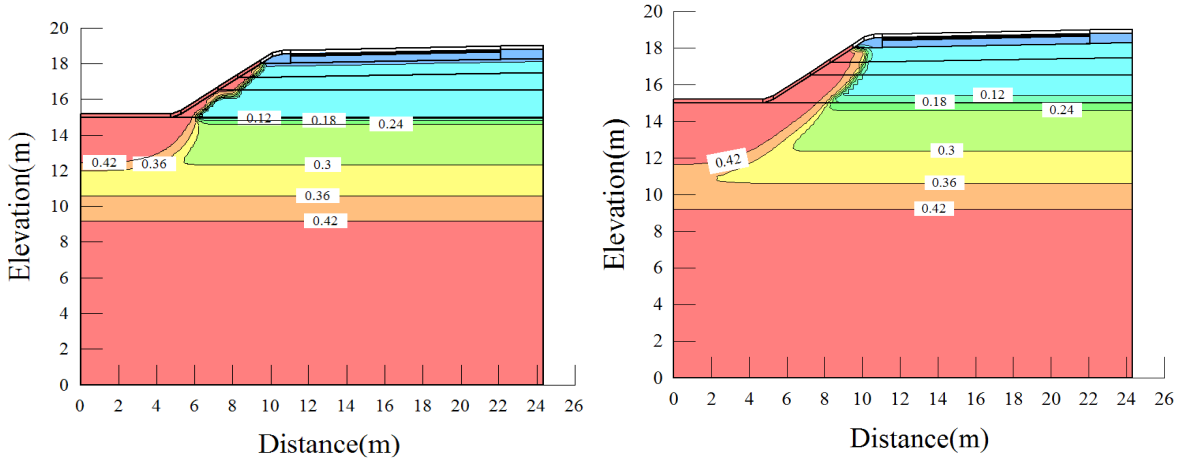

(a) (b)

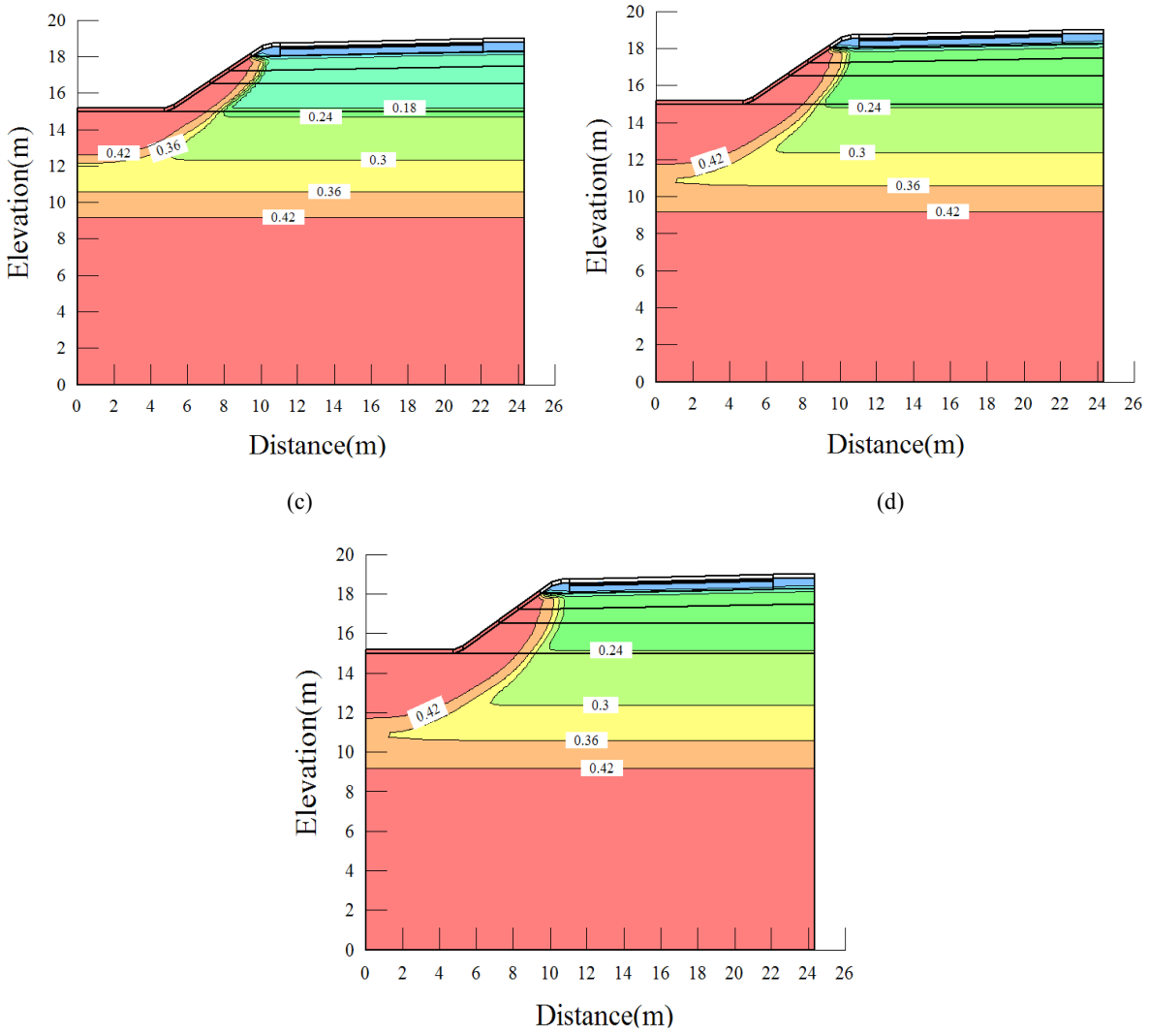

Fig. 3: Contours of subgrade humidity fields affected by initial humidity; (a): Initial humidity 3%; (b): Initial humidity 5%; (c): Initial humidity 7%; (d): Initial humidity 9%; (e): Initial humidity 11%

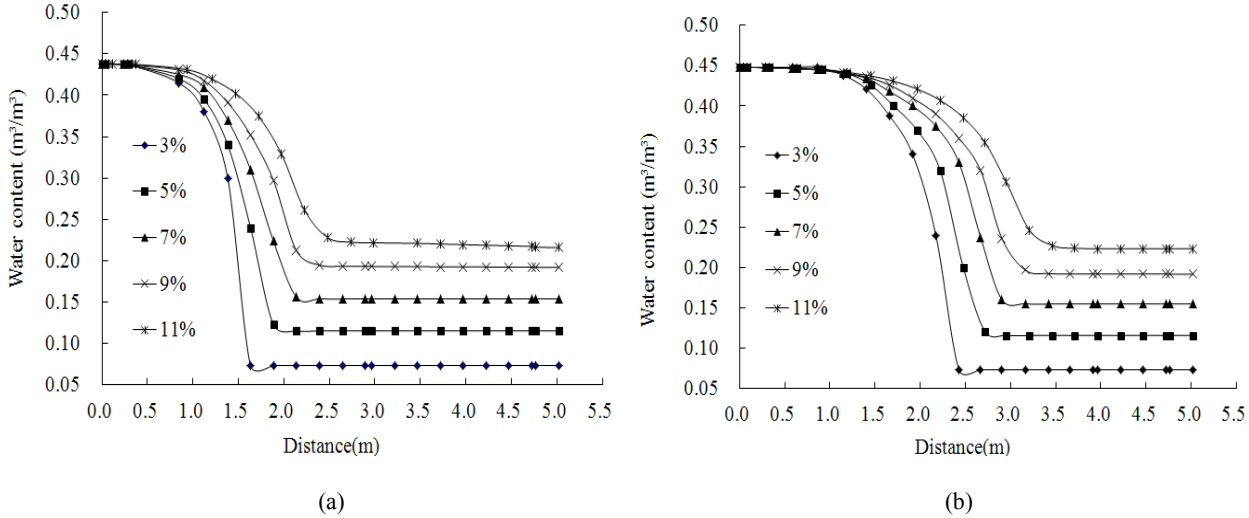

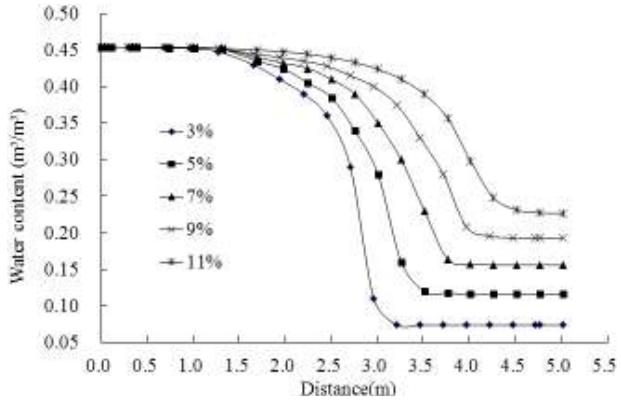

(c)

Fig. 4: Humidity distributions at test layers of subgrade; (a): Layer 30 cm; (b): Layer 120 cm; (c): Layer 250 cm

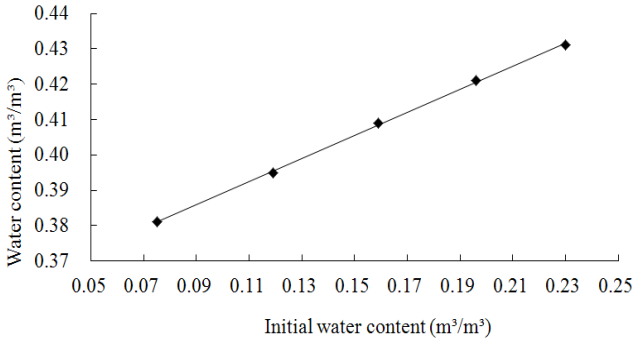

Fig. 5: Humidity and initial water content at 1.2 m below the subgrade

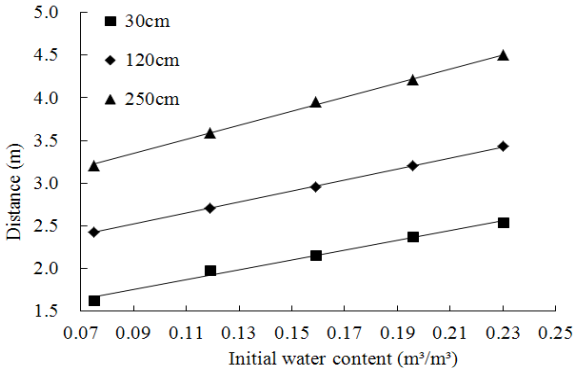

Fig. 6: Expansion of disturbed areas and the initial water content

same; this indicates that the surface humidity is not influenced by the initial subgrade humidity difference but by the rainfall intensity and duration (Liu, 2015). Besides the slope surface, the subgrade humidity increases with the increase of the initial water content at the same observation locations, the further the distance is, the larger the humidity increases. Figure 5 shows the humidity change at the location of 1.2 m depth.

It is seen in Fig. 5 that the humidity and the initial water content follows a linear relationship: $w_v = 0.33 \cdot w_{in} + 0.36$ ($R^2 = 0.99$), where w_{in} is the initial subgrade humidity (similarly hereinafter), m^3/m^3. Figure 4 also shows that the humidity differs as the depth of the measure points increases, as a result, the slope is larger.

Morphologic change of the disturbed area: The influence of the initial water content on the disturbed area is obvious. In Fig. 6, the disturbed area increases with the increase of the initial water content.

Figure 6 shows that the expansion of disturbed area increases along with the initial water content linearly: $D = a \cdot w_{in} + b$. This indicates that the expansion speed changes linearly with the initial water content due to the

Table 3: Equation parameters

Layer (cm)	*a*	*b*	R^2
30	5.73	1.24	0.99
120	6.46	1.94	0.99
250	8.28	2.60	0.99

Table 4: Equation parameters

Layer (cm)	*a*	*b*	R^2
30	0.75	-14.14	0.99
120	0.87	-15.59	0.99
250	0.89	-14.27	0.99

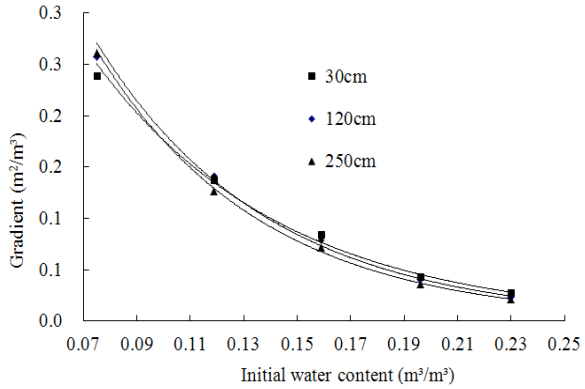

Fig. 7: The humidity gradient and the initial water content of the front disturbed area

same duration of rainfall. The larger the initial water content is, the faster the expansion speeds are. The larger the initial water contents are, the larger the initial infiltration coefficients are and the easier the moisture moves. The equation fitting of every layer are shown in Table 3.

The gradient of the front disturbed area: The whole disturbed area can be divided into the front area and the back area. The later area is close to the side of the slope with larger humidity and the decrease speed is lower, the gradient value is smaller (about 10% differs from the surface of the subgrade). While the front area is close to the side of the humidity forward with a trend opposite to the back area. The initial water content influences the states of the front disturbed area more, particularly in the difference of the humidity gradients. The humidity gradients change of the front disturbed area with the initial water content is shown in the Fig. 7.

Figure 7 shows that the humidity gradient decreases along with the increase of the initial water content following the rule of $G = a \bullet e^{b \bullet win}$, where G is the humidity gradient, m^2/m^3; The equation fitting of every layer are listed in Table 4.

CONCLUSION

In this study, the humidity distribution and change of the disturbed area of the subgrade, induced by rainfall infiltration have been investigated. The main conclusions are as follows:

- The humidity of the surface of the slope is not influenced by the initial subgrade humidity difference. Other than the slope surface, the humidity and the initial water content follows a linear relationship at the same observation location.
- Initial water content has a great influence on the distribution of the disturbed area. The expansion distance increases linearly as the initial water content increases. The larger the initial water contents are, the larger the initial infiltration coefficients are and the easier the moisture moves.
- The whole disturbed area can be divided into the front area and the back area. The later area is close to the side of the slope with larger humidity and the decrease speed is lower, the gradient value is smaller (about 10% differs from the surface of the subgrade). While the front area is close to the side of the humidity forward with a trend opposite to the back area. The initial water content influences the states of the front disturbed area more, particularly in the difference of the humidity gradients.

ACKNOWLEDGMENT

This study was supported by the Transportation Research Project of Jiangsu Province "The crack resistance and engineering application of the polyester fiber-reinforced cement-stabilized macadam base" (Grant No. 2014Y02G).

REFERENCES

Cho, S.E. and S.R. Lee, 2001. Instability of unsaturated soil slopes due to infiltration. Comput. Geotech., 28(3): 185-208.

Heydinger, A.G. and B.O.A. Davies, 2006. Analysis of Variations of Pavement Subgrade Soil Water Content. Geotechnical Special Publication No. 147, ASCE, 1: 247-257.

Liu, Z.J., 2012. The evolution of highway subgrade humidity field in westernarid and semi arid regions. Ph.D. Thesis, China University of Mining and Technology, Xuzhou. (In Chinese)

Liu, Z.J., 2014. Numerical study of subgrade humidity field evolution with different compaction models. J. Cent. South Univ., Sci. Technol., 45(4): 1341-1345. (In Chinese)

Liu, Z.J., 2015. Influence of rainfall characteristics on the infiltration moisture field of highway subgrades. Road Mater. Pavement, 16(3): 635-652.

Mahmood, K. and J.M. Kim, 2011. Reliability study of unsaturated embankment exposed to short duration rainfall pattern. Electron. J. Geotech. Eng., 16: 629-640.

Mahmood, K., J.H. Ryu and J.M. Kim, 2013. Effect of anisotropic conductivity on suction and reliability index of unsaturated slope exposed to uniform antecedent rainfall. Landslides, 10(1): 15-22.

Tarefder, R., N. Saha and J. Stormont, 2010. Evaluation of subgrade strength and pavement designs for reliability. J. Transp. Eng., 136(4): 379-391.

Zeng, L., H.Y. Fu, T. Li and Y.Q. Qin, 2012. The analysis of seepage characteristics and stability of carbonaceous mudstone embankment slope in rainfall condition. Adv. Mater. Res., 446-449: 1864-1868.

Zhang, H.B. and X.G. Song, 2011. Variation of moisture content and safety factor of silt subgrade under rainfall infiltration. Adv. Mater. Res., 243-249: 4161-4165.

Zuo, G., W. Wright, N. Randy Rainwater, E. Drumm and R. Yoder, 2002. Factors affecting determination of subgrade water content from multisegment time domain reflectometry probes. Transp. Res. Record, 1808(1): 3-10.